Effect of the inclusion of Galium in normal Cadmium chloride treatment on electrical properties of CdS/CdTe solar cell

OJO, A.A., OLUSOLA, I.O. and DHARMADASA, I <http://orcid.org/0000-0001-7988-669X>

EFFECT OF THE INCLUSION OF GALIUM IN NORMAL CADMIUM CHLORIDE TREATMENT ON ELECTRICAL PROPERTIES OF CdS/CdTe SOLAR CELL

A.A. Ojo*, I.O. Olusola and I.M. Dharmadasa

Electronic Materials and Sensors Group, Materials and Engineering Research Institute (MERI), Sheffield Hallam University, Sheffield S1 1WB, UK.

*Email: chartell2006@yahoo.com; Tel: +44 114 225 6910 Fax: +44 114 225 6930

ABSTRACT

The inclusion of gallium into the well-known $CdCl_2$ post-growth treatment shows drastic improvement in both CdTe material and electrical properties of the fully fabricated CdS/CdTe-based solar cell as compared with the regular $CdCl_2$ treatment. The optical, morphological, compositional and electronic properties the glass/FTO/n-CdS/n-CdTe/p-CdTe were explored after post-growth treatment of glass/FTO/n-CdS/n-CdTe/p-CdTe with $CdCl_2$ and $CdCl_2$:Ga treatments at 430 °C for 20 min. Morphological analysis show grain growths within the ranges of (100 – 2000) nm and (200 – 2600) nm for $CdCl_2$ and $CdCl_2$:Ga treatments as compared with the as-deposited glass/FTO/n-CdS/n-CdTe/p-CdTe layer with grain size within the ranges of (100 – 250) nm. Structurally, the preferred orientation of the as-deposited CdTe remains (111)C after both $CdCl_2$ and $CdCl_2$:Ga treatments of glass/FTO/n-CdS/n-CdTe/p-CdTe with randomisation of crystallite orientation observed after $CdCl_2$:Ga with an increase in the diffraction intensities of the (220)C and (311)C CdTe peaks. The multilayer structure glass/FTO/n-CdS/n-CdTe/p-CdTe utilised in this work was grown using electrodeposition technique. The glass/FTO/n-CdS/n-CdTe/p-CdTe sample was divided into three sets; the first and second sets were treated with $CdCl_2$ and $CdCl_2$:Ga respectively, while the third set was left as-deposited. Both the $CdCl_2$ and $CdCl_2$:Ga sets were heat treated in air at 430°C for 20 min, etched to improve metal/semiconductor interface and metallised with 100 nm Au contacts. The current-voltage measurements show comparative improvements in the open-circuit voltage, short-circuit current density, fill factor and the solar cell efficiency of the $CdCl_2$:Ga treated glass/FTO/n-CdS/n-CdTe/p-CdTe as compared with the $CdCl_2$ treated structure. A conversion efficiency of ~11% was achieved with the $CdCl_2$:Ga treatment while ~7% was achieved with the $CdCl_2$ treatment of similar glass/FTO/n-CdS/n-CdTe/p-CdTe device structure. This observation shows that the inclusion of gallium further improves $CdCl_2$ treatment of CdS/CdTe-based solar cell due to its unique features of improving the stoichiometry of the CdTe layer.

1 INTRODUCTION

Heterojunction solar cell formed by the combination of semiconductors from groups II and VI, with emphasis on cadmium sulphide/cadmium telluride (CdS/CdTe) based solar cell have been considered as an alternative to silicon (Si) based solar cell [1], [2]. CdS/CdTe-based solar cell which has attained 21.5% conversion efficiency [3] can be deposited using different techniques as reported in the literature [1]. Post-growth treatment (PGT) has been considered as an integral part of achieving highly efficient solar cell [4]. This is justified by recrystallisation and grain growth, optimisation of electrical conductivity and doping concentration, passivation of grain boundaries, optimisation of the CdS/CdTe interface morphology, improvement in Cd:Te stoichiometric composition, reduction of Te precipitation amongst other advantages observed after PGT in the presence of some halogen based salts and gases [5]–[9]. As documented in the literature, it is challenging to completely avoid the presence of Te precipitates in CdTe by modifying the growth technique, growth process or post-growth treatment [10]–[12]. Fernandez, 2003, discussed that the presence of Te precipitates is attributed to peculiarities of the CdTe phase diagram [13] with Te-rich composition in the vicinity of melting point and a strong retrograde character of solidus on Te-rich side of homogeneity region [14]. Dharmadasa et al, 2015 [11] relate the incorporated defects within CdTe bandgap at 0.40±0.04 eV, 0.65±0.02 eV and the broad mid-gap defect level at 0.73±0.02 eV within the CdTe bandgap (1.45 eV) to Te-richness, while, the defects at 0.96±0.04 and 1.18±0.02 were related to Cd-richness in CdTe layers using photoluminescence (PL) study. Defects related to Cd-rich CdTe are more useful when large Schottky barriers are required at the CdTe/metal interface in achieving high performing devices. This has also been demonstrated by Burst et al, 2016 [15] and Reese et al, 2015 [16]. Other independent researchers have established the reduction of defect concentrations of CdTe at 0.40±0.04 eV, 0.65±0.02 eV and 0.73±0.02 using PL study [13] by annealing CdTe in gallium melt. Therefore, Ga has a unique property of reducing Te-richness in CdTe material. Based on this understanding, this work focuses on the effect of the inclusion of shallow donor dopant such as gallium into the normal cadmium chloride post-growth treatment as it affects both the material and device properties of CdS/CdTe-based solar cell.

2 2. EXPERIMENTAL DETAILS

All the chemicals and substrates used in this work were procured from Sigma Aldrich, UK. Two-electrode electrodeposition configuration was utilised in this work for its simplicity and minimised contamination route. Fluorine-doped tin oxide (FTO) substrates with sheet resistance ~7 Ω/□ were used as the working electrode while high purity carbon rod was utilised as the anode. The substrate was cut into 4×3 cm^2 and attached to a

cathode using polytetrafluoroethylene (PTFE) tape. Computerised GillAC potentiostat was utilised as the power supply source. Prior to deposition, the working electrode was cleaned in an ultrasonic bath containing soap solution and rinsed in deionised (DI) water. Afterwards, the substrate was degreased using acetone and later rinsed in a flow of DI water before been transferred into the electrolytic bath. It should be noted that all the cathodic potentials utilised in this work have been pre-characterised, optimised and published [17], [18].

2.1 Sample preparation

2.1.1 CdS bath preparation and growth

120 nm thick cadmium sulphide (CdS) was cathodically electrodeposited on the glass/FTO substrate from an aqueous electrolyte containing cadmium chloride hydrate ($CdCl_2 \cdot xH_2O$) of 98% purity and ammonium thiosulphate $(NH_4)_2S_2O_3$ 99% purity. The salt concentrations of 0.12M $CdCl_2 \cdot xH_2O$ and 0.18M $(NH_4)_2S_2O_3$ in 800 ml deionised (DI) water was utilised. The solution was contained in a 1000 ml polypropylene beaker while the beaker was placed in an 1800 ml glass beaker containing DI water. The glass beaker serves as the outer bath containing a low volume of DI water to maintain uniform heating of the electrolyte within the inner polypropylene container. The outer beaker was heated using a programmable hot plate/stirrer system with the stirring rate set to ~300 rpm. Prior to the deposition of CdS, the electrolytic system was adjusted to pH 2.00±0.02 and the bath temperature was maintained at ~85˚C during growth. The bath was electro-purified for ~30 hours prior to the deposition of CdS. The CdS layer was deposited at an optimised cathodic potential of 1200 mV based on structural, optical, morphological, compositional and electrical property analysis [17].

Immediately after growth, the glass/FTO/CdS was rinsed in flowing DI water to wash off loose elemental Cd and S on the CdS layer. The layer was dried under a nitrogen stream and heat treated at 400˚C for 20 minutes in air to improve the characteristic properties of CdS [5]. The inclusion of $CdCl_2$ was avoided at this stage to isolate the effect of $CdCl_2$ and $CdCl_2$+$Ga_2(SO_4)_3$ on the post-growth treatment of glass/FTO/n-CdS/n-CdTe/p-CdTe layers.

2.1.2 CdTe bath preparation and growth

CdTe was electrochemically deposited on well rinsed and heat treated glass/FTO/CdS substrate in an electrolytic bath containing cadmium nitrate tetrahydrate ($Cd(NO_3)_2 \cdot 4H_2O$) of 99.98% purity and tellurium oxide (TeO_2) of 5N (99.999%) purity. Salt concentrations of 1.5M $Cd(NO_3)_2 \cdot 4H_2O$ and 5 ml of dissolved TeO_2 solution were contained in 800 ml DI water. Due to the insolubility of TeO_2 in water, 0.03M TeO_2 was prepared

by dissolving 2g of TeO_2 in 30 ml concentrated nitric acid. The acidic solution was stirred continuously for 60 minutes prior to its dilution with 400 ml of DI water. The tellurium concentration in the electrolytic bath was kept low due to the high difference in the reduction potential of Cd and Te.

The pH at the start of electrodeposition and growth temperature of the bath were adjusted to 2.00±0.02 and ~85˚C respectively. The outer glass beaker setup as explained for the CdS bath was also utilised. 1100 nm thick *n*-type CdTe layer was grown at 1370 mV on the glass/FTO/n-CdS substrate. Afterwards, ~30 nm of *p*-CdTe was deposited on *n*-CdTe layer using the same electrolytic bath. This was achieved by adjusting the growth voltage to 1360 mV in a continuous growth process. The incorporation of the thin p-CdTe layer is for the formation of a *p*-*n* junction at *n*-CdTe/*p*-CdTe interface with very low lattice mismatch and an Ohmic contact on the Au/*p*-CdTe interface [14], minimise the contact resistance [19], enhance the band bending by pinning the Fermi level (FL) close to the valence band as later shown in Figure 6 (b) and improve the reproducibility of the devices. Although pinning the FL close to the valence band can be achieved through surface etching as demonstrated in the literature [20], [21], the back layer Cd/Te concentration in this work was altered as explained in Section 2.1.2, so that only the thin CdTe layer (~30 nm) is *p*-type while the bulk of the CdTe layer (~1100 nm) remains n-type after PGT as demonstrated by Salim et al, 2015 [18]. It should be that under ideal conditions, the incorporated p-CdTe back layer is expected to pin the Fermi level close to the valence band whereby higher barrier height can be formed. Conversely, the incorporation of p-CdTe introduces defect related to Te-richness in CdTe [22]. For this reason, it is essential that the thickness of the p-CdTe back layer is optimised.

The glass/FTO/*n*-CdS/*n*-CdTe/*p*-CdTe layer was rinsed in DI water and dried in a stream of nitrogen afterwards. The 4×3 cm^2 glass/FTO/*n*-CdS/*n*-CdTe/*p*-CdTe was divided into 3 sets of 4×1 cm^2, labelled AD (as-deposited), CCT ($CdCl_2$ treated) and GCT ($CdCl_2$:Ga treated) based on the post-growth treatment undergone.

2.1.3 Post-growth treatment preparation and application

In this study, two aqueous solutions (A and B) were used to treat the material layers. Solution A contains 0.1M $CdCl_2$ in 20 ml of DI water at room temperature, while solution B contains 0.1M $CdCl_2$ and 0.05M $Ga_2(SO_4)_3$ in 20 ml of DI water at room temperature. The solutions were stirred continuously for 1 hour to achieve homogeneity. The sample labelled AD was left as-deposited, while samples labelled CCT and GCT were $CdCl_2$ treated in solution A and $CdCl_2$:Ga treated in solution B respectively.

The application of $CdCl_2$ and $CdCl_2$+$Ga_2(SO_4)_3$ on the grown glass/FTO/*n*-CdS/*n*-CdTe/*p*-CdTe was achieved by adding few drops of relevant solution on the glass/FTO/*n*-CdS/*n*-CdTe/*p*-CdTe surface. The full coverage of the glass/FTO/n-CdS/n-CdTe/p-CdTe layer with the treatment solutions was achieved with a damped cotton bud. Both the CCT and GCT treated glass/FTO/n-CdS/n-CdTe/p-CdTe layers were allowed to air-dry before heat treatment. The heat treatment was performed at 430˚C for 20 minutes in air atmosphere for samples undergoing each treatment based on previously optimised conditions [4], [23]–[25]. The CCT and GCT treated glass/FTO/n-CdS/n-CdTe/p-CdTe layers were then rinsed in DI water and dried in a stream of nitrogen afterwards. It should be noted that the incorporation of gallium in CdTe reduced the intensity of the cathodoluminescence (CL) peak associated with defects in CdTe [13]. Therefore the addition of Ga in the regular $CdCl_2$ treatment will further reduce defects in CdTe, improve the stoichiometry and perhaps dope the material.

The surfaces of the AD, CCT and GCT glass/FTO/*n*-CdS/*n*-CdTe/*p*-CdTe layers were etched using a solution containing $K_2Cr_2O_7$ and concentrated H_2SO_4 for acid etching and a solution containing NaOH and $Na_2S_2O_3$ for basic etching for 2 seconds and 2 minutes respectively to improve the metal/semiconductor contact [26], [27]. Immediately afterwards, the (AD, CCT and GCT) samples were transferred to a high vacuum system in order to deposit 2 mm diameter and 100 nm thick Au contacts on the glass/FTO/*n*-CdS/*n*-CdTe/*p*-CdTe structure. The fabricated devices were analysed using current-voltage characteristic measurements to determine their device parameters.

2.2 Characterisation techniques

The information about the level of crystallinity and phase identification of deposited layers were obtained using Philips PW 3710 X'pert diffractometer with Cu-Kα monochromator of wavelength λ=1.54 Å. The X-ray generator tension and current were adjusted respectively to 40 kV and 40 mA for these experiments. The optical properties of the grown thin films were studied at room temperature using Cary 50 Scan Ultraviolet-Visible (UV-Vis) spectrophotometer within the wavelength range of (200 – 1000) nm. The morphological and compositional analyses of the deposited layers were studied using FEI Nova 200 NanoSEM equipment. The electrical conductivity type of the layers was determined using Photoelectrochemical (PEC) cell measurements. The fully fabricated solar cell parameters were measured using fully automated Rera Solution I-V measurement system.

3 RESULTS AND DISCUSSION

3.1 Analysis of CdS layer

Although this work is mainly based on the effect of post-growth treatment (PGT) as it affects the CdTe absorber layer but the basic characteristics of the underlying CdS layer will be briefly discussed. Figure 1 (a) shows a graph of the square of the absorption against photon energy, while Figures 1 (b) and 1 (c) show the typical SEM micrograph and XRD patterns of heat treated CdS layer. As shown in Figure 1 (a), the bandgap of the electrodeposited CdS layer utilised in this work is ~2.42 eV. This was derived by taking the tangent of the straight line portion of the curve at the photon energy value at A^2=0. The observed bandgap is comparable to the bulk CdS bandgap.

From observation, the SEM micrograph of CdS as depicted in Figure 1 (b) shows a full coverage of the underlying glass/FTO substrate. Due to the good coverage, shunting paths between FTO and the CdTe top layer is substantially sealed off. The observation of small grain justifies CdS wetting property. Furthermore, the electrodeposited CdS utilised in this work is polycrystalline in nature as observed in Figure 1 (c) with a preferred orientation along hexagonal (101) plane.

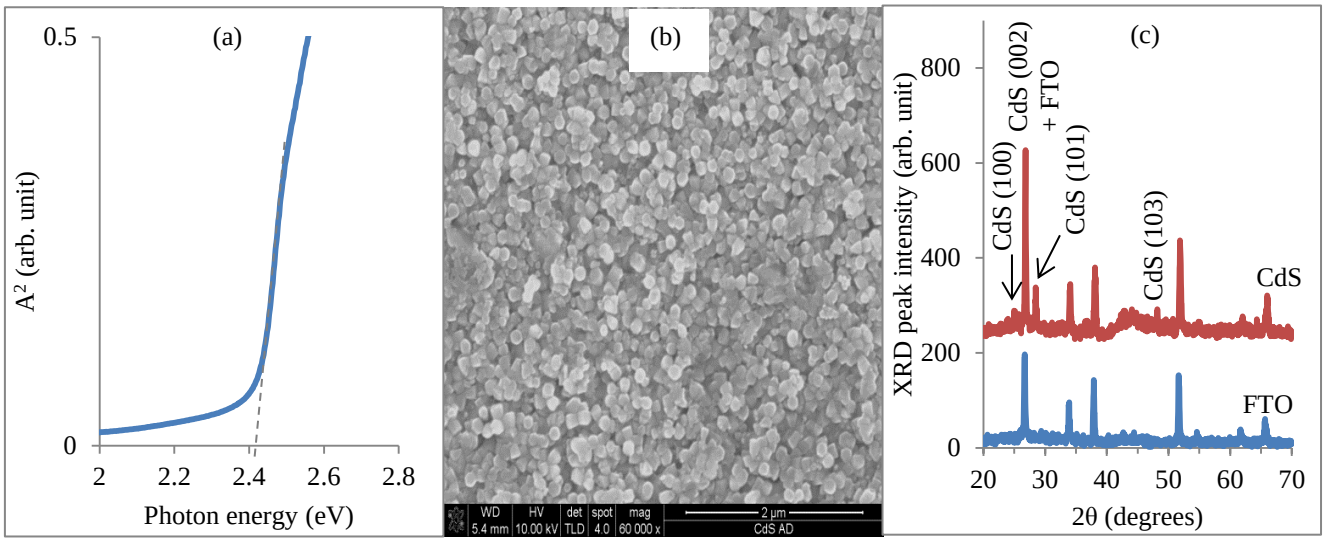

Figure 1: Typical (a) optical absorption curve, (b) SEM micrograph and (c) XRD spectrum of heat treated CdS layers grown by electroplating.

3.2 Analysis of CdS/CdTe layers

3.2.1 Optical absorption analysis

Figure 2 (a) shows the optical absorption curves, while Figure 2 (b) shows the slope of the absorption edges and bandgaps for AD, CCT and GCT - glass/FTO/*n*-CdS/*n*-CdTe/*p*-CdTe layers. As observed in Figures 2 (a) and 2 (b), the bandgap of all the AD, CCT and GCT layers falls within the CdTe bulk bandgap range of (1.45 to 1.50) eV [28], even for the as-deposited layer without any PGT to modify its optical parameters. Although, there were no clear differences in the bandgap due to the material quality of the as-deposited CdTe layer, the difference in the absorption edge is clearly observed in Figure 2 (b). Bosio et al, (2006) reported that the sharpness of the absorption edge signifies superior semiconductor layer optical property [5]. Based on this submission, it could be interpreted that the layer with the superior optical quality is the GCT layer and the least is the as-deposited CdTe layer. It is interesting to observe an inverse relationship (see Figure 2 (b)) between the bandgap and the absorption edge slope which further buttresses the GCT - glass/FTO/*n*-CdS/*n*-CdTe/*p*-CdTe material superiority.

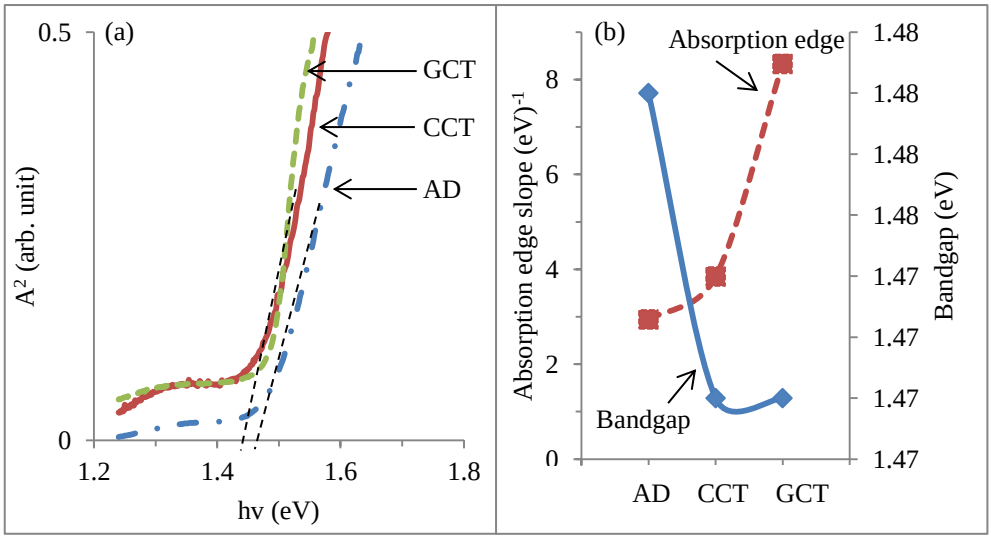

Figure 2: Graphs of (a) Square of absorption against photon energy and (b) Optical bandgap and slope of absorption edge against treatment conditions for AD, CCT and GCT - glass/FTO/n-CdS/n-CdTe/p-CdTe layers.

Table 1: Summary of the effect of different treatments on bandgap and the slope of absorption edges.

Sample	Bandgap (eV)	Absorption edge slope (eV^{-1})
AD	1.48	2.94
CCT	1.47	3.85
GCT	1.47	8.33

3.2.2 Morphological analysis

Figures 3 (a), 3 (b) and 3 (c) show the morphology of AD, CCT and GCT - glass/FTO/*n*-CdS/*n*-CdTe/*p*-CdTe thin films. As observed from Figure 3, the underlying substrates are fully covered by the CdTe layer before and after different treatments. The as-deposited glass/FTO/*n*-CdS/*n*-CdTe/*p*-CdTe layer shows agglomeration of small crystallites to form cauliflower-like larger grains. After post-growth treatment such as CCT and GCT, grain growths within the range of (100 – 2000) nm and (200 – 2600) nm were observed respectively. The influence of $CdCl_2$ in PGT of CdTe has been explicitly explored in the literature as it affects the improvement of material and device quality of CdTe based solar cells [4]–[6]. Further improvements in grain size can be observed in morphological property of the GCT treated glass/FTO/*n*-CdS/*n*-CdTe/*p*-CdTe layer as shown in Figure 3 (c) as compared with the CCT in Figure 3 (b) in this work. Although this improvement signals the positive effect of the inclusion of Ga in the usual CCT of CdTe, it cannot be ascertained at this stage.

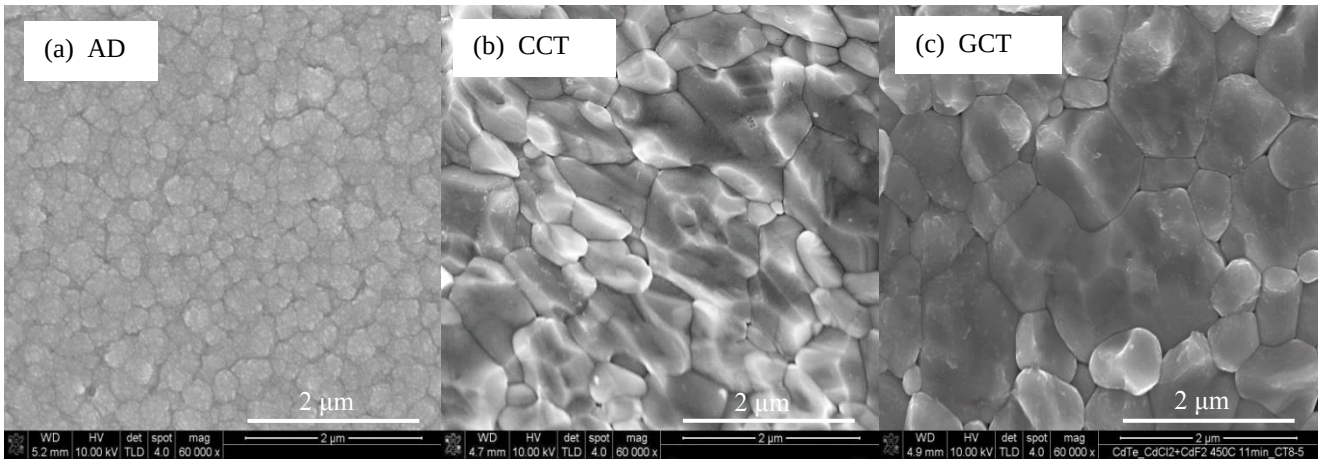

Figure 3: Typical SEM micrographs of (a) AD, (b) CCT and (c) GCT CdTe thin films electrodeposited on CdS layer at 1370 mV.

3.2.3 Compositional analysis

Figure 4 shows the atomic composition of a typical glass/FTO/*n*-CdS/*n*-CdTe/*p*-CdTe multilayer configuration as detected by EDX technique. It should be noted that in addition to Cd and Te, the presence of S, Si, Sn and F may also be observed due to underlying glass/FTO/CdS substrate, Cl or Ga due to the PGT utilised and O due to layer oxidation. As expected, low Cd/Te composition was observed for the AD layer due to the Te-richness during the growth of the top *p*-CdTe layer at lower cathodic potential. This observation further buttresses the fact that provided CdTe is not subjected to any extrinsic doping, the conductivity type of CdTe is composition dependent for the as-deposited layer as later shown in Section 3.2.5. A shift towards unity of Cd/Te ratio was observed after CCT and GCT. This observation has been reported in the literature [4]–[6], [18] as one of the advantages of PGT of CdTe. It should be noted that in addition to elemental composition, self-compensation and

doping effect can take place during PGT. In the case of GCT, the presence of gallium can also remove Te-precipitate during the heat treatment [13], [19]. Therefore, the combination of all these processes seems to produce beneficial properties for the CdTe layer and the glass/FTO/*n*-CdS/*n*-CdTe/*p*-CdTe structure.

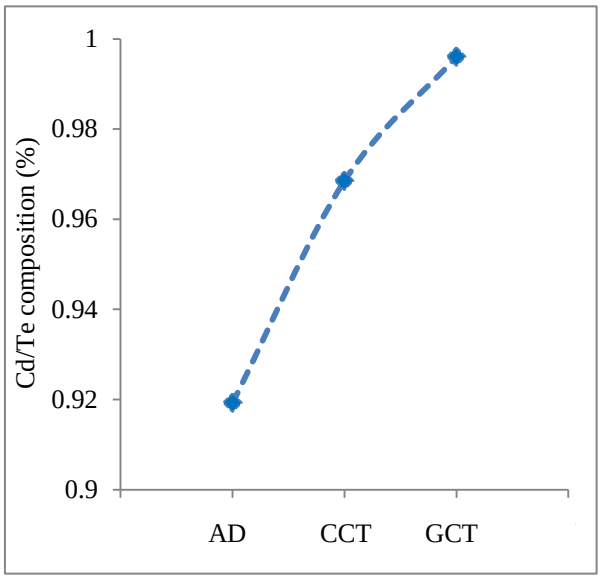

Figure 4: Percentage composition ratio of Cd to Te atoms in a glass/FTO/n-CdS/n-CdTe/p-CdTe configuration after different PGT.

3.2.4 Structural analysis

Figure 5 shows the structural analysis of electrodeposited glass/FTO/*n*-CdS/*n*-CdTe/*p*-CdTe layers under different conditions and Table 2 summarises the results of X-ray diffraction (XRD) analysis on the effect of different post-growth treatments on glass/FTO/n-CdS/n-CdTe/p-CdTe layers. It was observed that no reflection can be attributed to the underlying CdS layer [29] except for the hexagonal CdS (002) which coincides with the FTO peak at angle 2θ=26.68˚ cannot be ascertained. Other reflections attributed to FTO were observable at 2θ=32.9°, 37.1° and 51.6°. XRD reflections assigned to cubic (111), (220) and (311) CdTe phases at 2θ=23.88°, 38.65° and 45.84° were also observed. It can be deduced from Figure 5 that under all conditions explored in this work, the most intense XRD reflection is observed at 2θ=23.85°. For the CCT - glass/FTO/n-CdS/n-CdTe/p-CdTe layer, an increase in the cubic (111)C orientation was observed as compared to AD without any observable change in the other CdTe reflections. However, for GCT - glass/FTO/n-CdS/n-CdTe/p-CdTe layer, randomisation of crystallite orientation was observed. This is usually seen with the collapse of (111) peak and increase in (220) and (311) peaks. As reported recently [30], these changes suddenly occurs when the grain boundaries are melted due to presence of impurities such as excess Cd, Cl, O and Ga. The presence of Ga seems to enhance the decrease in the (111) peak and increasing the (220) and (311) peak intensities due to randomisation of crystal orientations.

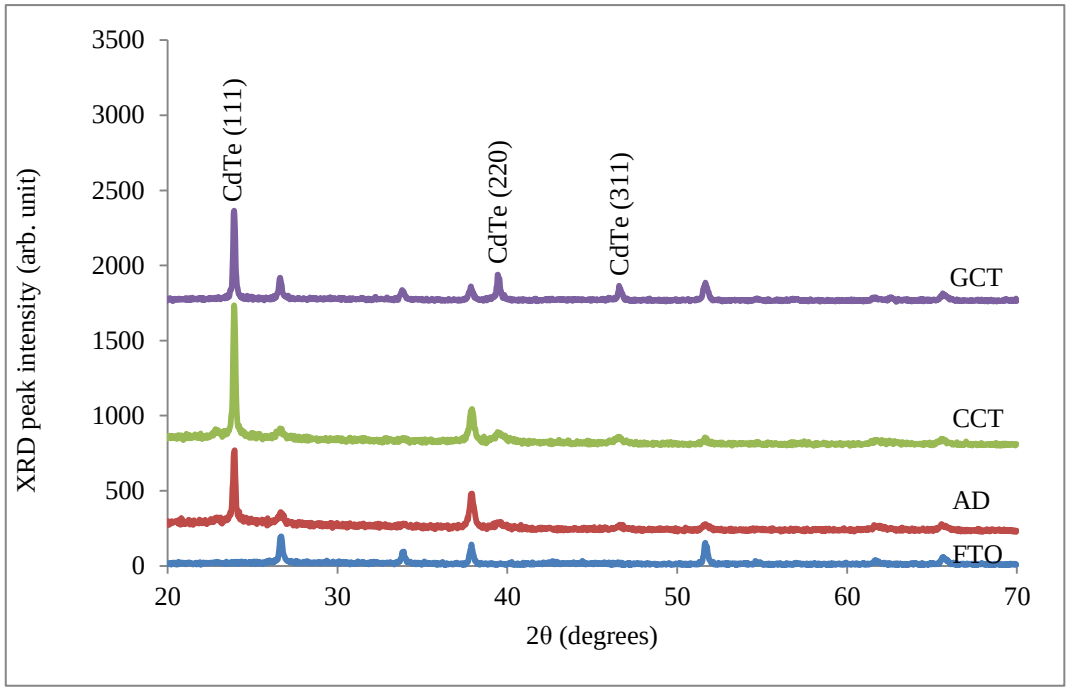

Figure 5: XRD spectra of glass/FTO/n-CdS/n-CdTe/p-CdTe structures for different conditions (AD, CCT and GCT).

From the comparison between the AD, CCT and GCT glass/FTO/n-CdS/n-CdTe/p-CdTe layers, it could be inferred that the inclusion of gallium in the normal cadmium chloride treatment PGT may have triggered the re-crystallisation and reorientation of the crystalline planes in this work. It should be noted that alterations in XRD patterns also depends on the underlying substrates and heat treatment conditions used [30].

As shown in Table 2, there was no clear distinction between the glass/FTO/n-CdS/n-CdTe/p-CdTe layers explored in this work as concerning the full-width-at-half-maximum (FWHM), lattice spacing and crystallite size calculated using Scherrer equation. This observation might be due to the limitations of the use of Scherrer equation [31] or the XRD analysis software on polycrystalline material layers with large crystals.

Table 2: The XRD analysis on the effect of PGT on CdTe layers.

Treatment	2θ (degrees)	Lattice spacing (Å)	FWHM (degrees)	Crystallite size D (nm)	Plane (hkl)	Assignments
AD	23.94	3.72	0.162	52.3	(111)	Cubic
CCT	23.92	3.72	0.162	52.3	(111)	Cubic
GCT	23.92	3.72	0.162	52.3	(111)	Cubic

3.2.5 Photoelectrochemical (PEC) cell study

The PEC cell requires the formation of a solid/liquid junction between a semiconductor and a suitable electrolyte. The electrolyte utilised in this work is 0.1 M sodium thiosulphate ($Na_2S_2O_3$). Both the semiconductor and a counter electrode (high purity carbon rod) introduced to the electrolyte are connected to a voltmeter. Band bending at the semiconductor/electrolyte interface forms a Schottky type potential barrier due to the equalisation of the FL of both the semiconductor and the electrolyte. The direction of band bending is determined by the conductivity type of the semiconductor. The voltage difference (V_L-V_D) under illuminated (V_L) and dark (V_D) conditions determines the conductivity type of the semiconductor [32]. It should be noted that the use of PEC as against other robust conductivity measurement techniques such as Hall Effect measurement is pertinent due to the underlying conducting substrate FTO.

Table 3 shows the PEC signal of glass/FTO/*p*-CdTe layer after different PGTs. It was observed that the *p*-conduction type of the as-deposited CdTe layer was retained after different treatments. Although, a shift in the PEC signal towards the *n*-type conduction region was also observable in both the CCT and GCT *p*-CdTe layers.

Table 3: PEC cell measurements on p-CdTe layers after different treatments

Sample	V_L (mV)	V_D (mV)	PEC signal (V_L-V_D) (mV)	Conductivity type
AD	-61	-84	23	P
CCT	-78	-96	18	p
GCT	-42	-47	5	p

This observation depicts the movement of the FL which was close to the valence band towards the middle of the bandgap due to the alteration in doping as a result of the heat treatment condition [6], Cd/Te compositional changes [33] amongst other factors. Other incorporated layers such as *n*-CdS and *n*-CdTe have been known to retain their conductivity type with a slight shift towards the opposite conductivity type [17], [18].

3.3 Solar cell devices characterisation

Based on the analysis as discussed in Section 3.2.5, the glass/FTO/n-CdS/n-CdTe/p-CdTe layer schematics and the band diagram can be represented by Figure 6 (a) and Figure 6 (b) respectively.

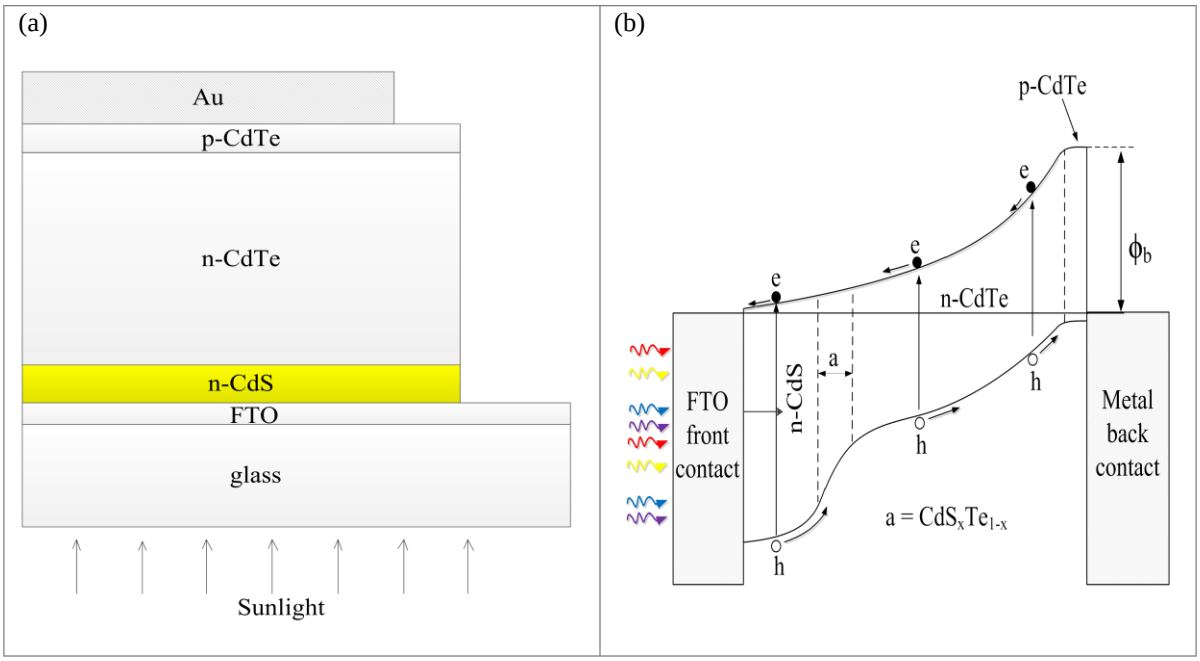

Figure 6: (a) Schematic diagram and (b) The band diagram of the glass/FTO/n-CdS/n-CdTe/p-CdTe/Au thin film solar cell.

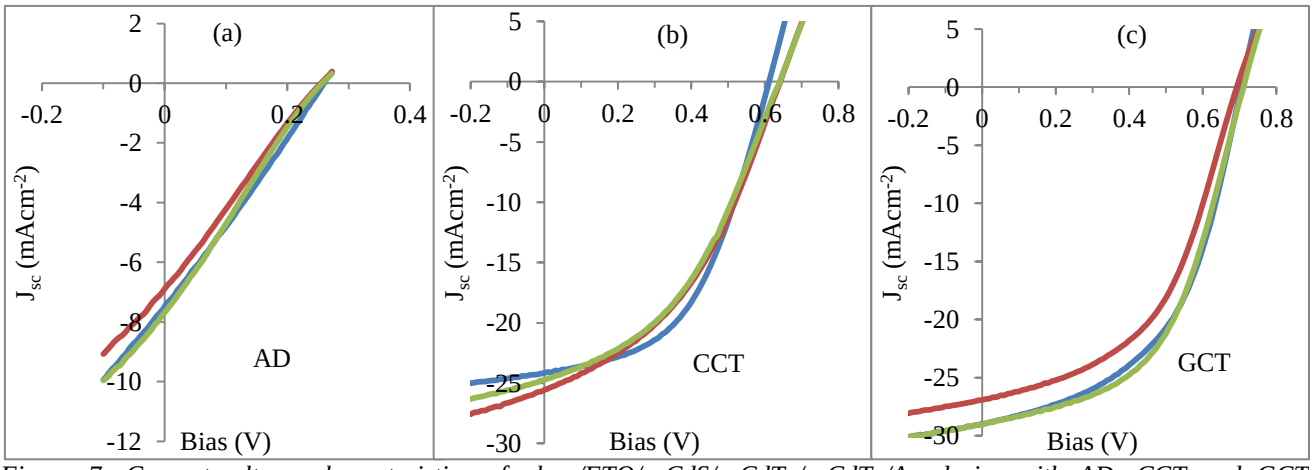

Figure 7: Current-voltage characteristics of glass/FTO/n-CdS/n-CdTe/p-CdTe/Au devics with AD, CCT and GCT conditions.

Figures 7 (a), 7 (b) and 7 (c) shows the current-voltage (I-V) curves of glass/FTO/*n*-CdS/*n*-CdTe/*p*-CdTe/Au layers with different PGT conditions, measured under AM1.5 as discussed in Section 2.2. From these I-V curves measured under illuminated condition, solar cell parameters such as series resistance (R_s), shunt resistance (R_{sh}), short-circuit current density (J_{sc}), open-circuit voltage (V_{oc}), fill factor (*FF*) and conversion efficiency (η) can be determined. Experimentally observed solar cell parameters for the different conditions are summarised in Table 4 for three champion cells. Both the series resistance R_s and shunt resistance R_{sh} were calculated from the slopes

inverse of the linear-linear I-V curve in the forward and reverse bias respectively under AM 1.5 illuminated condition.

The high R_s and low R_{sh} values as observed in the fabricated solar cell incorporating AD - CdTe can be directly attributed to low semiconductor material quality as described by Soga, 2004 [34]. It is clearly observed in Figure 7 and Table 4 that the improvement in the electrical properties of the glass/FTO/*n*-CdS/*n*-CdTe/*p*-CdTe/Au devices can be achieved after some chlorine based treatment [35]. The addition of gallium into the regular $CdCl_2$ treatment further enhances the device performance. This enhancement can be attributed to the material properties improvement after treatment and as discussed in Section 3.2. It should be noted that the short-circuit current density as observed in this work is higher than the Shockley–Queisser limit on single *p*-*n* junction [36] as a result of the incorporation of the multilayer *n*-*n*-*p* configuration [37]. The structure represents an early stage of graded bandgap, multilayer devices configuration.

Table 4: Tabulated device parameters obtained from I-V measurements under A.M1.5 illuminated condition.

Treatment	R_s (Ω)	$R_{sh} \times 10^3$ (Ω)	J_{sc} (mAcm^{-2})	V_{oc} (V)	Fill factor	Efficiency (%)
AD	1027	1.4	7.1	0.25	0.24	0.43
	1062	1.5	7.8	0.26	0.24	0.49
	1180	1.3	7.6	0.25	0.24	0.46
CCT	302	6.4	24.2	0.61	0.50	7.50
	353	3.8	25.5	0.64	0.43	7.01
	354	3.2	24.8	0.64	0.43	6.84
GCT	273	8.0	29.9	0.72	0.52	11.21
	319	7.1	27.4	0.70	0.52	9.97
	276	8.0	29.3	0.73	0.52	11.12

Furthermore, the comparatively higher *FF*, J_{sc} and V_{oc} observed with cells fabricated using GCT CdTe solar cells can be attributed to the incorporation of *n*-dopant treatment such as gallium in CdTe by the introduction of excess electron into the crystal lattice to boost conductivity and also further improvement in the material quality as observed in Sections 3.2.1 to 3.2.5. Similar observations have been recorded in the literature with the incorporation of *n*-dopant to CdTe [38]–[40]. Although the effect of the incorporation of gallium on bandgap defects cannot be depicted from the I-V results, the improvement in the overall electronic properties of the fabricated devices is observable.

4 CONCLUSION

The effect of the inclusion of Ga to the regular $CdCl_2$ post-growth treatment on the material and electronic properties of CdS/CdTe based layers has been explored in this work. The optical analysis shows that the grown

CdTe layer is within the standard bulk CdTe bandgap range with material superiority after $CdCl_2$:Ga treatment due to the steeper absorption edge slope. The morphological studies show full material coverage and grain growth after both CCT and GCT. The compositional analysis shows the improvement of stoichiometry when treated with GCT. The structural analysis shows improvement in the XRD peak intensity reflection of the as-deposited glass/FTO/*n*-CdS/*n*-CdTe/*p*-CdTe after both CCT and GCT with the preferred orientation along the cubic (111) plane. Although, more pronounced recystallisation was observed after GCT with a comparative reduction in the (111)C and an increase in the (220)C plane, showing improvement of grain boundary enhanced PV effect.

Improvement in the electrical properties of the fabricated glass/FTO/*n*-CdS/*n*-CdTe/*p*-CdTe/Au was observed after PGT with GCT showing better results than CCT owing to the gallium inclusion in the treatment. With further material optimisation of gallium doping in CdTe treatment, improved electronic properties can be achieved. Work is on-going on the optimisation of Ga concentration and treatment parameter required for this inclusion.

ACKNOWLEDGEMENT

The main author would like to thank Sheffield Hallam University, Ekiti State University, TETFund Nigeria for their support to carry out this research programme.

REFERENCES

[1] T. M. Razykov, C. S. Ferekides, D. Morel, E. Stefanakos, H. S. Ullal, and H. M. Upadhyaya, "Solar photovoltaic electricity: Current status and future prospects," *Prog. Sol. Energy 1*, vol. 85, no. 8, pp. 1580–1608, 2011.

[2] S. G. Kumar and K. S. R. K. Rao, "Physics and chemistry of CdTe/CdS thin film heterojunction photovoltaic devices: fundamental and critical aspects," *Energy Environ. Sci.*, vol. 7, no. 1, pp. 45–102, 2014.

[3] "First Solar raises bar for CdTe with 21.5% efficiency record: pv-magazine." [Online]. Available: http://www.pv-magazine.com/news/details/beitrag/first-solar-raises-bar-for-cdte-with-215-efficiency-record_100018069/#axzz3rzMESjUl. [Accessed: 20-Nov-2015].

[4] I. M. Dharmadasa, "Review of the CdCl2 Treatment Used in CdS/CdTe Thin Film Solar Cell Development and New Evidence towards Improved Understanding," *Coatings*, vol. 4, no. 2, pp. 282–307, 2014.

[5] A. Bosio, N. Romeo, S. Mazzamuto, and V. Canevari, "Polycrystalline CdTe thin films for photovoltaic applications," *Prog. Cryst. Growth Charact. Mater.*, vol. 52, no. 4, pp. 247–279, 2006.

[6] B. M. Başol, "Processing high efficiency CdTe solar cells," *Int. J. Sol. Energy*, vol. 12, no. 1–4, pp. 25–35, 1992.

[7] H. Liu, Y. Tian, Y. Zhang, K. Gao, K. Lu, R. Wu, D. Qin, H. Wu, Z. Peng, L. Hou, and W. Huang, "Solution processed CdTe/CdSe nanocrystal solar cells with more than 5.5% efficiency by using an inverted device structure," *J. Mater. Chem. C*, vol. 3, no. 17, pp. 4227–4234, 2015.

[8] H. Xue, R. Wu, Y. Xie, Q. Tan, D. Qin, H. Wu, and W. Huang, "Recent Progress on Solution-Processed CdTe Nanocrystals Solar Cells," *Appl. Sci.*, vol. 6, no. 7, p. 197, 2016.

[9] A. A. Dharmadasa, I.M., Echendu, O.K, Fauzi, F, Abdul-Manaf, N.A., Olusola, O.I., Salim, H.I., Madugu, M.L., Ojo, "Improvement of composition of CdTe thin films during heat treatment in the presence of CdCl2," *J Mater Sci Mater Electron*, no. Submitted, pp. 1–10, 2016.

[10] J. C. Tranchart and P. Bach, "A gas bearing system for the growth of CdTe," *J. Cryst. Growth*, vol. 32, no. 1, pp. 8–12, Jan. 1976.

[11] I. M. Dharmadasa, O. K. Echendu, F. Fauzi, N. A. Abdul-Manaf, H. I. Salim, T. Druffel, R. Dharmadasa, and B. Lavery, "Effects of CdCl2 treatment on deep levels in CdTe and their implications on thin film solar cells: a comprehensive photoluminescence study," *J. Mater. Sci. Mater. Electron.*, vol.

26, no. 7, pp. 4571–4583, 2015.

[12] N. V. V Sochinskii, V. N. N. Babentsov, N. I. I. Tarbaev, M. D. Serrano, and E. Dieguez, "The low temperature annealing of p-cadmium telluride in gallium-bath," *Mater. Res. Bull.*, vol. 28, no. 10, pp. 1061–1066, 1993.

[13] P. Fernández, "Defect structure and luminescence properties of CdTe based compounds," *J. Optoelectron. Adv. Mater.*, vol. 5, no. 2, pp. 369–388, 2003.

[14] K. Zanio, *Semiconductors and semimetals*, vol. 13. New York: Academic Press, 1978.

[15] J. M. Burst, J. N. Duenow, D. S. Albin, E. Colegrove, M. O. Reese, J. A. Aguiar, C.-S. Jiang, M. K. Patel, M. M. Al-Jassim, D. Kuciauskas, S. Swain, T. Ablekim, K. G. Lynn, and W. K. Metzger, "CdTe solar cells with open-circuit voltage breaking the 1V barrier," *Nat. Energy*, no. February, p. in press, 2016.

[16] M. O. Reese, C. L. Perkins, J. M. Burst, S. Farrell, T. M. Barnes, S. W. Johnston, D. Kuciauskas, T. A. Gessert, and W. K. Metzger, "Intrinsic surface passivation of CdTe," *J. Appl. Phys.*, vol. 118, no. 15, 2015.

[17] N. A. Abdul-Manaf, A. R. Weerasinghe, O. K. Echendu, and I. M. Dharmadasa, "Electro-plating and characterisation of cadmium sulphide thin films using ammonium thiosulphate as the sulphur source," *J. Mater. Sci. Mater. Electron.*, vol. 26, no. 4, pp. 2418–2429, 2015.

[18] H. I. Salim, V. Patel, a. Abbas, J. M. Walls, and I. M. Dharmadasa, "Electrodeposition of CdTe thin films using nitrate precursor for applications in solar cells," *J. Mater. Sci. Mater. Electron.*, vol. 26, no. 5, pp. 3119–3128, 2015.

[19] J. M. Woodcock, A. K. Turner, M. E. Ozsan, and J. G. Summers, "Thin film solar cells based on electrodeposited CdTe," in *The Conference Record of the Twenty-Second IEEE Photovoltaic Specialists Conference - 1991*, 1991, pp. 842–847.

[20] I. M. Dharmadasa, a B. McLean, M. H. Patterson, and R. H. Williams, "Schottky barriers and interface reactions on chemically etched n-CdTe single crystals," *Semicond. Sci. Technol.*, vol. 2, no. 7, pp. 404–412, Jul. 1987.

[21] S. Tanaka, J. A. Bruce, and M. S. Wrighton, "Deliberate modification of the behavior of n-type cadmium telluride/electrolyte interfaces by surface etching. Removal of Fermi level pinning," *J. Phys. Chem.*, vol. 85, no. 25, pp. 3778–3787, Dec. 1981.

[22] I. M. Dharmadasa, J. D. Bunning, a. P. Samantilleke, and T. Shen, "Effects of multi-defects at

metal/semiconductor interfaces on electrical properties and their influence on stability and lifetime of thin film solar cells," *Sol. Energy Mater. Sol. Cells*, vol. 86, no. 3, pp. 373–384, 2005.

[23] O. I. Olusola, "Optoelectronic devices based on graded bandgap structures utilising electroplated semiconductors," Sheffield Hallam University, 2016.

[24] H. I. Salim, "Multilayer Solar Cells Based on CdTe Grown From Nitrate Precursor, PhD Thesis, Sheffield Hallam University, UK," 2016.

[25] O. K. Echendu, "Thin film solar cells using all-electrodeposited ZnS , CdS and CdTe materials," 2014.

[26] I. M. Dharmadasa, C. J. Blomfield, C. G. Scott, R. Coratger, F. Ajustron, and J. Beauvillain, "Metal/n-CdTe interfaces: A study of electrical contacts by deep level transient spectroscopy and ballistic electron emission microscopy," *Solid. State. Electron.*, vol. 42, no. 4, pp. 595–604, Apr. 1998.

[27] I. M. Dharmadasa, "Recent developments and progress on electrical contacts to CdTe, CdS and ZnSe with special reference to BARRIER contacts to CdTe," *Prog. Cryst. Growth Charact. Mater.*, vol. 36, no. 4, pp. 249–290, Jan. 1998.

[28] T. L. Chu and S. S. Chu, "Thin film II–VI photovoltaics," *Solid. State. Electron.*, vol. 38, no. 3, pp. 533–549, Mar. 1995.

[29] T. Toyama, K. Matsune, H. Oda, M. Ohta, and H. Okamoto, "X-ray diffraction study of CdS/CdTe heterostructure for thin-film solar cell: Influence of CdS grain size on subsequent growth of (111)-oriented CdTe film," *J. Phys. D. Appl. Phys.*, vol. 39, no. 8, pp. 1537–1542, 2006.

[30] I. Dharmadasa, P. Bingham, O. Echendu, H. Salim, T. Druffel, R. Dharmadasa, G. Sumanasekera, R. Dharmasena, M. Dergacheva, K. Mit, K. Urazov, L. Bowen, M. Walls, and a. Abbas, "Fabrication of CdS/CdTe-Based Thin Film Solar Cells Using an Electrochemical Technique," *Coatings*, vol. 4, no. 3, pp. 380–415, 2014.

[31] A. Monshi, "Modified Scherrer Equation to Estimate More Accurately Nano-Crystallite Size Using XRD," *World J. Nano Sci. Eng.*, vol. 2, no. 3, pp. 154–160, 2012.

[32] J. Nowotny, T. Bak, M. Nowotny, and L. Sheppard, "Titanium dioxide for solar-hydrogen I. Functional properties☆," *Int. J. Hydrogen Energy*, vol. 32, no. 14, pp. 2609–2629, 2007.

[33] T. M. Razykov, N. Amin, B. Ergashev, C. S. Ferekides, D. Y. Goswami, M. K. Hakkulov, K. M. Kouchkarov, K. Sopian, M. Y. Sulaiman, M. Alghoul, and H. S. Ullal, "Effect of CdCl2 treatment on physical properties of CdTe films with different compositions fabricated by chemical molecular beam deposition," *Appl. Sol. Energy*, vol. 49, no. 1, pp. 35–39, 2013.

[34] T. Soga, “Nanostructured Materials for Solar Energy Conversion,” *Elsvier Sci.*, vol. 2030, p. 614, 2004.

[35] J. D. Major, R. E. Treharne, L. J. Phillips, and K. Durose, “A low-cost non-toxic post-growth activation step for CdTe solar cells,” *Nature*, vol. 511, no. 7509, pp. 334–337, Jun. 2014.

[36] W. Shockley and H. J. Queisser, “Detailed Balance Limit of Efficiency of p-n Junction Solar Cells,” *J. Appl. Phys.*, vol. 32, no. 3, p. 510, 1961.

[37] A. De Vos, “Detailed balance limit of the efficiency of tandem solar cells,” *J. Phys. D. Appl. Phys.*, vol. 13, no. 5, pp. 839–846, 2000.

[38] S. Mazzamuto, L. Vaillant, A. Bosio, N. Romeo, N. Armani, and G. Salviati, “A study of the CdTe treatment with a Freon gas such as CHF2Cl,” *Thin Solid Films*, vol. 516, no. 20, pp. 7079–7083, Aug. 2008.

[39] T. Ferid and M. Saji, “Transport properties in gallium doped CdTe MOVPE layers,” *J. Cryst. Growth*, vol. 172, no. 1–2, pp. 83–88, 1997.

[40] T. L. Chu, S. S. Chu, C. Ferekides, J. Britt, and C. Q. Wu, “Thin-film junctions of cadmium telluride by metalorganic chemical vapor deposition,” *J. Appl. Phys.*, vol. 71, no. 8, pp. 3870–3876, 1992.

TABLE OF FIGURES